

NOTICE

THIS DOCUMENT HAS BEEN REPRODUCED FROM
MICROFICHE. ALTHOUGH IT IS RECOGNIZED THAT
CERTAIN PORTIONS ARE ILLEGIBLE, IT IS BEING RELEASED
IN THE INTEREST OF MAKING AVAILABLE AS MUCH
INFORMATION AS POSSIBLE

(NASA-TM-81066) APPLICATION OF A
MULTI-LEVEL GRID METHOD TO TRANSONIC FLOW
CALCULATIONS (NASA) 30 p HC A03/MF A01

N80-25054

CSCL 12A

Unclassified
G3/64 18098

I CASE REPORT

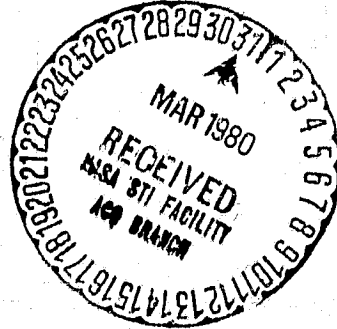
APPLICATION OF A MULTI-LEVEL GRID METHOD TO TRANSONIC FLOW CALCULATIONS

Jerry C. South, Jr.

Achi Brandt

Report Number 76-8

March 19, 1976



INSTITUTE FOR COMPUTER APPLICATIONS

IN SCIENCE AND ENGINEERING

Operated by the

UNIVERSITIES SPACE RESEARCH ASSOCIATION

at

NASA'S Langley Research Center

Hampton, Virginia

APPLICATION OF A MULTI-LEVEL GRID METHOD
TO TRANSONIC FLOW CALCULATIONS*

Jerry C. South, Jr.^{**}
NASA Langley Research Center
Hampton, Virginia

and

Achi Brandt^{***}
Weizmann Institute of Science
Rehovot, ISRAEL

SUMMARY

A multi-level grid method has been studied as a possible means of accelerating convergence in relaxation calculations for transonic flows. The method employs a hierarchy of grids, ranging from very coarse (e.g. 8 x 2 mesh cells) to fine (e.g. 128 x 32); the coarser grids are used to diminish the magnitude of the smooth part of the residuals, hopefully with far less total work than would be required with, say, optimal SLOR iterations on the

* This research, partially supported by NASA Grant NGR-47-102-001, was initiated while Dr. Brandt was visiting ICASE (Institute for Computer Applications in Science and Engineering) at Langley Research Center.

** Assistant Head, Theoretical Aerodynamics Branch

*** Professor of Mathematics, currently on leave at IBM Research Center, Mathematics Dept., Yorktown Heights, New York.

finest grid. The method was applied to the solution of the transonic small-disturbance equation for the velocity potential in conservation form. Nonlifting transonic flow past a parabolic-arc airfoil is the example studied, with meshes of both constant and variable step size.

INTRODUCTION

The multi-level grid method, for accelerating convergence in relaxation calculations, has been shown to be very efficient for solving elliptic problems with Dirichlet boundary conditions. For background and historical material, see references 1 to 4. In reference 5, Brandt gives an extensive discussion and analysis of the method, together with several different procedures for applying the method. The idea of the method is based on the fact that in many typical elliptic boundary-value problems, the error is composed of a discrete spectrum of wave lengths, which range from the width of the region down to the width of a mesh cell. The short wave-length components of the error are usually diminished quite rapidly in a relaxation calculation, while the long wave-length components diminish very slowly. After only a few iterations the residual will be smooth, since the short wave-length error components have been eliminated; and thus the residual can be represented accurately on a coarser mesh. An equation called the "residual" equation is then solved on the coarser mesh, and the resulting correction is added to the last approximation on the fine mesh, yielding a significant improvement with very little work.

Since relaxation methods are currently the most attractive for obtaining numerical solutions to transonic aerodynamics problems, the question arises as to whether a multi-level, or multi-grid (MG) method can be used in a mixed

flow with shock waves. In this paper we report some early results using the MG method to solve a simple transonic problem: we consider the transonic small-disturbance equation for the velocity potential, for nonlifting flow past a parabolic-arc airfoil.

PROBLEM DESCRIPTION

The transonic small-disturbance equation for the velocity potential can be written in conservation form as:

$$p_x + q_y = 0 \quad (1)$$

where

$$p = \left[K - \frac{(\gamma + 1)}{2} M_\infty^2 \phi_x \right] \phi_x \quad (2)$$

$$q = \phi_y \quad (3)$$

$$K = (1 - M_\infty^2) / \tau^{2/3} \quad (4)$$

Equation (1) is to be solved subject to the boundary conditions that the disturbance potential, ϕ , vanishes at infinity and the flow is tangent to the airfoil surface, in the interval $|x| \leq 1/2$; i.e.,

$$\begin{aligned} \text{at } y = 0, \quad & \phi_y = F'(x) \quad \text{for } |x| \leq 1/2 \\ & = 0 \quad \text{for } , \quad |x| > 1/2 \end{aligned} \quad (5)$$

where $F(x)$ is the (upper surface) thickness distribution function.

τ is the usual thickness ratio, and γ , M_∞ , and K are the ratio of specific heats, free-stream Mach number, and transonic similarity parameter, respectively. The form of equations (1) to (5) is a correctly-scaled transonic similarity form, in that all quantities are of order 1. Physical quantities, denoted by a "hat" symbol are related to the scaled quantities as follows:

$$\begin{aligned}
 \hat{\phi} &= c\tau^{2/3}\phi \\
 \hat{x} &= cx \\
 \hat{y} &= c\tau^{-1/3}y \\
 \hat{t}(x) &= 2c\tau F(x)
 \end{aligned} \tag{6}$$

where c is the airfoil chord length and \hat{t} is the total thickness distribution of the symmetric airfoil.

Equation (1) is of hyperbolic or elliptic type depending on whether

$$U = K - (\gamma + 1) M_\infty^2 \phi_x \tag{7}$$

is negative or positive, respectively.

Finite-Difference Equations

Murman's conservative difference scheme (ref. 6) can be conveniently presented in terms of Jameson's "switching function" (ref. 7) as follows:

$$(1 - \mu_{ij}) p_{ij} + \mu_{i-1,j} p_{i-1,j} + q_{ij} = 0 \tag{8}$$

where

$$p_{ij} = u_{ij} \frac{\phi_{i+1,j} - 2\phi_{ij} + \phi_{i-1,j}}{\Delta x^2} \tag{9}$$

$$u_{ij} = K - (\gamma + 1) M_\infty^2 \frac{\phi_{i+1,j} - \phi_{i-1,j}}{2\Delta x} \tag{10}$$

$$q_{ij} = \frac{\phi_{i,j+1} - 2\phi_{ij} + \phi_{i,j-1}}{\Delta y^2} \tag{11}$$

(12)

and where

$$\begin{aligned}\mu_{ij} &= 0 && \text{if } U_{ij} > 0 \\ &= 1 && \text{if } U_{ij} \leq 0\end{aligned}\tag{12}$$

It should be noted here that, in the interest of simplicity, we have presented only the constant-step-size (unstretched grid) form of the difference equations. In the case of a stretched grid, the conservative difference equations cannot be factored into the nice form given above, but this presents no real difficulty. The actual computer program is written for a stretched grid, with the identity transformation (constant step size) included as a special case.

Vertical Line Relaxation

A vertical line relaxation scheme for solving equation (8) by iteration can be written as:

$$AT_{i,j-1} + BT_{ij} + CT_{i,j+1} = R_{ij} + DT_{i-1,j} + ET_{i-2,j}\tag{13}$$

where $T_{ij} = \phi_{ij}^+ - \phi_{ij}$ (14)

ϕ^+ denotes a "new" value of ϕ , obtained during the latest iteration sweep, while ϕ is the value from the previous sweep. R_{ij} , which is the left-hand side of equation (8), is evaluated with "old" values of ϕ_{ij} , as are the iteration coefficients A through E, which are given in the appendix.

Multi-Grid Approach

Let us introduce a sequence of grids G_1, G_2, \dots, G_M , where for simplicity, $h_k = 2h_{k+1}$, and h_k represents the step size of the G_k grid. We can represent the iteration operator (e.g., eq. (13)) on the finest grid G_M as:

$$L_M(\phi_M) = f_M \quad (15)$$

where ϕ_M is the exact discrete solution on the G_M grid. We can write

$$\phi_M = u_M + v_M \quad (16)$$

where u_M is the approximate solution and v_M is the error. Then we have the residual equation:

$$\begin{aligned} \bar{L}_M(v_M) &= f_M - L_M(u_M) \\ &= -R_M \end{aligned} \quad (17)$$

where R_M is the residual of the approximation u_M on the G_M grid. \bar{L}_M is in general different from L_M in the nonlinear case, which complicates matters. Nevertheless, if R_M is smooth, the error will be smooth, and the residual equation (17) can be solved on a coarser grid. Thus, for example, we can write

$$\bar{L}_{M-1}(w_{M-1}) = I_M^{M-1}(R_M) \quad (18)$$

where w is an approximation to the error v_M on the G_{M-1} grid, and I_k^ℓ denotes interpolation from the G_k to G_ℓ . After solving the problem (18) (usually with homogeneous boundary conditions), we interpolate the function w_{M-1} back onto the G_M mesh, and thus form an improved approximation:

$$(u_M)_{\text{new}} = (u_M)_{\text{old}} + I_{M-1}^M(w_{M-1}) \quad (19)$$

In the complete MG algorithm, the solution of equation (18) is also

performed by relaxation; and if the convergence rate falls below a prescribed level, we can apply a similar procedure, backing up to the G_{M-2} grid level, and so on, until we arrive at G_1 , if necessary. The G_1 grid is so coarse that a direct solution could be used economically, but we have used iteration here also.

Full Approximation - In the general nonlinear case, the form of the operator \bar{L} can be quite complicated — more so than the original operator, L — and thus applications to, say, the full potential equation may be tedious to program. It turns out that for the transonic small disturbance equation, the job is simple, and our first program did use the exact expression for \bar{L} in an efficient way. However, there is an equivalent, easier method for solving the residual equation, which we call the full approximation method, as follows:

Suppose we add to both sides of equation (18) the function

$$L_{M-1}(u_M) - f_{M-1} = \tilde{R}_{M-1} \quad (21)$$

Then, since $\bar{L}_{M-1}(w_{M-1}) + L_{M-1}(u_M) \approx L_{M-1}(\phi_M)$,

we have

$$L_{M-1}(\phi_M) \approx \tilde{R}_{M-1} - I_M^{M-1}(R_M) \quad (22)$$

We can now use the original operator on all the grids, which greatly simplifies the programming. The right-hand side of equation (22) is the difference between the residuals of u_M calculated with the coarse-and fine-grid operators.

Note that when the solution converges on the G_M grid, then

$$R_M \rightarrow 0 \quad (23a)$$

$$I_M^{M-1}(R_M) \rightarrow 0 \quad (23b)$$

but \tilde{R}_{M-1} will remain finite, since ϕ_M is a solution on the G_M grid; \tilde{R}_{M-1} is essentially the truncation error of the L_{M-1} operator.

After equation (22) is solved to sufficient accuracy, we determine the function

$$w_{M-1} = \phi_M - I_M^{M-1} (u_M) \quad (24)$$

by subtraction at all points of the grid G_{M-1} , and then interpolate w_{M-1} to the G_M grid as before in equation (19).

More explicit details of the method will be deferred to a forthcoming report.

RESULTS AND DISCUSSION

In order to estimate the efficiency of the method, a work unit can be defined as the amount of computational effort required for one relaxation sweep on the (finest) G_M grid. Thus a relaxation sweep on the G_k grid costs $n_w = (1/4)^{M-k}$ work units, for example. Likewise, when we calculate the residuals for the G_k grid, we perform these calculations at the points of the G_{k-1} grid, i.e., 1/4 as few points; hence each residual calculation costs less than 1/4 the effort of a relaxation sweep on the G_k grid, or approximately $(1/4)^{M-k+1}$. Note that this is an overestimate, since the tridiagonal system (13) is not inverted, nor do we calculate the iteration coefficients during the residual calculations. On the other hand we did not count the work of interpolation in equation (19), for example, or any other "overhead" of that type.

An overall estimate of efficiency can be given by the number

$$a = \left\{ \frac{\|R_{M,n_w}\|}{\|R_{M,1}\|} \right\}^{1/n_w} \quad (25)$$

where

$$\|R_M, 1\| = \text{norm of } R_M \text{ after first sweep on } G_M$$

$$\|R_M, n_w\| = \text{norm of } R_M \text{ after } n_w \text{ work units}$$

and

$$\|R_M\| = (\Delta x \Delta y \sum_{ij} R_M^2)^{1/2} \quad (26)$$

Hence the norm we use is the root mean square of the residual on G_M . This number is typically about 5 to 10 times smaller than the maximum norm in transonic problems. We consider an approximate solution to be converged when

$$\|R_M\| < C/(\text{no. of grid points}) \quad (27)$$

where the prescribed constant C is typically chosen as 1 so as to estimate the nominal truncation error.

Unstretched Grids

In the case of a grid with constant steps in both directions, the present MG method performed quite well. In the following some typical results are summarized. All of the figures shown are copies of the screen display, on a remote computer terminal, of an abbreviated history of the MG runs. The first integer is the grid level, M , corresponding to G_M in our text. The next three "E"-format numbers are:

1. $\max_{ij} |R_{ij}|$ (See equation (13)).

2. $\|R_M\|$ (See equation (26)).

3. $\max_{ij} |T_{ij}|$ (See equation (14)).

The two integers following 1. above are the i,j location where the $\max_{ij} |R_{ij}|$

occurred. The last two numbers in a row are the number of work units, n_w , and the number of supersonic points. One row is printed for each relaxation sweep on the finest (G_M) grid, but not for the coarser grids. However, each time the calculation "backs up" to a coarser grid, the words RESCAL are printed and the value of $\max_{ij} |R_{ij}|$ and $\|R_M\|$ are printed, together with the grid level(L) which has just been relaxed. Note that these norms correspond to $I_M^{M-1}(R_M)$ in the right-hand side of equation (22). In all MG runs shown, a relaxation factor of 1.0 was used on all grids. Likewise all MG runs in these examples used five levels of grids ($M = 5$), with G_1 being 4×2 mesh cells in the x -and y -directions, respectively, and G_5 being a 64×32 . We have done 6 levels, with G_6 being 128×64 with no deterioration in MG performance.

Laplace's Equation. - To show just how fast the MG method works for a nice, smooth, elliptic problem, we present a run in figures 1 and 2 for Laplace's equation with the prescribed normal derivative equal to $\sin \pi x$ along $y = 0$. In figure 1, the convergence history is shown for G_4 , a 32×16 grid, and according to equation (25), we achieved $a = .540$. Now because of the smoothness of the solution, it may be expected that interpolating the converged G_4 solution onto G_5 will give a very good starting approximation for G_5 . This is true, as can be seen on figure 2, where the G_5 grid was started with the interpolated G_4 solution. For G_5 , we obtained $a = .583$, but the efficiency of the two combined levels is more like $a = .46$!

Figure 3 shows the convergence history for the same problem, using SLOR all the way on G_5 , achieving convergence in $n_w = 141$, yielding $a = .924$.

Nonlinear, Subcritical Flow ($M_\infty = 0.7$). - In figure 4 is shown the history of a nonlinear, but subcritical flow solved by MG. Here the convergence rate is the same or better, on G_5 , as it was for Laplace's equation with smooth boundary conditions discussed previously (i.e., $a = .549$). In this case, however, the Neumann boundary condition is an "N-wave" -- far from smooth -- and hence we can conclude that discontinuous boundary conditions do not deteriorate MG performance. SLOR, with $\omega = 1.85$, achieved $a = .868$.

Supercritical Flow ($M_\infty = .85$). - Figure 5 illustrates the history for a typical supercritical flow with a moderate-sized supersonic region. Since the G_5 grid has 2145 grid points, the supersonic region, with 124 points, occupies about 6% of the grid. For this case, $a = .593$. The same case using SLOR all the way converged in $n_w = 68$, using a relaxation factor of 1.85, and the $a = .855$.

Highly Supercritical Flow ($M_\infty = .95$). - Figure 6 illustrates the history for a highly supercritical flow, where the shock wave is at the trailing edge of the airfoil. Note the final number of supersonic points (355) is established after 38 work units. It is typical that, at that point, the MG method begins to work best, since most of the high frequency error components have been eliminated. For this case, $a = .858$, achieving convergence in 67.6 work units. The same case was converged with SLOR all the way in 228 work units, with $a = .957$.

Stretched Grids

We found quickly that vertical line relaxation alone is not the best way to relax the solution in the MG mode in the case of a stretched grid. A possible explanation for this is that all of the high-frequency error

components are not rapidly damped by vertical line relaxation in a general stretched mesh, where the mesh aspect ratio varies from very small to very large values. For if we consider the line relaxation algorithm for Laplace's equation, with a local mesh aspect ratio equal to A , and a relaxation factor ω , the amplification factor is:

$$g(\theta_x, \theta_y; A, \omega) = \frac{A [2(1-\omega) + \omega e^{i\theta_x}]}{A(2 - \omega e^{-i\theta_x}) + 2\omega(1 - \cos \theta_y)} \quad (28)$$

If $A = (\Delta y / \Delta x)^2$ is large, we have a problem, for then, with $\theta_x = 0$ and $\theta_y = \frac{\pi}{2}$,

$$\text{we have } g(0, \frac{\pi}{2}; A, \omega) = \frac{A(2-\omega)}{A(2-\omega) + 2\omega} \quad (29)$$

and if $\omega = 1$, we see that

$$|g| \rightarrow 1 \text{ as } A \rightarrow \infty$$

Clearly, choosing $\omega \approx 2$ alleviates the problem, but then other high-frequency components are retarded, i.e., for $\theta_x = \frac{\pi}{2}$ and $\theta_y = 0$,

$$|g(\frac{\pi}{2}, 0; A, \omega)| = \sqrt{\frac{4(1-\omega)^2 + \omega^2}{4 + \omega^2}} \quad (30)$$

which approaches 1 as ω nears 2.0. A solution to this problem is to sweep in all directions alternately (forward, backward, up, and down, in a general problem), but of course special care must be taken in supersonic regions.

Figure 7 shows an MG run with vertical line relaxation for the $M_\infty = .95$ flow, with the grid stretched to infinity in both the x - and y -directions. A logarithmic stretch was used, with 30% of the grid points in the x -direction

on the airfoil chord. Note that the maximum residual tends to occur far above the airfoil (small values of j), where $\Delta y / \Delta x$ is large. For this case, $a = .936$. The same case, solved by SLOR takes about 382 cycles to converge ($a = .974$). Some benefit is still achieved from the MG mode of operation; even though the MG performance is far worse than what we believe can be obtained by a better relaxation algorithm.

Since this last case is a particularly interesting flow, we have included some pictures of the output for the pressure distribution along $y = 0$ (Fig. 8), a chart of the Mach numbers in the computational plane (Fig. 9) and an isobar plot (Fig. 10). Note in figure 8 that an oblique shock occurs at the trailing edge, followed by a nearly-constant velocity supersonic zone in the wake, then a normal shock in the wake about 1/2-chord behind the trailing edge, and finally a very slow recovery to free-stream conditions. The airfoil lies between $I = 24$ and 42 ($x < .5$). Figures 9 and 10 show the "fishtail" shock pattern more clearly. In figure 9, only odd values of J are printed in order to fit the picture on the screen. $J = 1$ corresponds to infinity, as do $I = 1$ and 65 ; The values of I are the first column of integers, and the Mach numbers $\times 100$ are shown in the array. Flow is from top to bottom in the picture, with the line $y = 0$ (and the airfoil surface) on the left ($J = 33$, see bottom row of integers indicating the value of J). The isobar plot, figure 10, uses integers for supersonic flow values. The triangular region of nearly-constant velocity between the oblique shock at the trailing edge and the normal shock in the wake is clearly evident.

A summary of all these results is shown in figure 11.

CONCLUDING REMARKS

The multigrid (MG) method for accelerating relaxation calculations has been shown to be applicable to transonic flow with embedded shock waves. In this paper, vertical line relaxation was used for solving the nonlinear, conservative difference equation modelling the small-disturbance equation for the velocity potential. The multigrid approach appears to work about three to five times faster than optimal SLOR on unstretched grids of moderate size (64 x 32); The relative advantage of MG to SLOR increases as the grid gets finer, since the MG convergence rate is nearly independent of mesh size.

On stretched grids, the present MG method slows down, being only about twice as fast as SLOR. It is felt that the reason for this is clear; the indicated remedy being alternating-direction relaxation sweeps.

Future investigations will include the alternating sweeps, and the extension of the method to lifting flows.

ACKNOWLEDGEMENT

During the course of this work, Professor Antony Jameson of the Courant Institute of Mathematical Sciences, New York University, also carried out research on the multigrid method. He showed independently that the "Full Approximation" approach would work. Our many discussions have been beneficial.

Langley Research Center
National Aeronautics and Space Administration
Hampton, VA 23665
February 4, 1976

APPENDIX

Iteration Coefficients

We have used various choices for iteration coefficients in equation (13).

The coefficients used to make the calculations presented in this paper are simply based on the Newton linearization of equations (8), (9), and (11). They are as follows:

First define: (dropping the j index, since all quantities are evaluated at the same j)

$$b_{i+\frac{1}{2}} = \left[K - (\gamma+1) N_\infty^2 \frac{(\phi_{i+1} - \phi_i)}{\Delta x} \right] \Delta x^{-2} \quad (A1)$$

Then we have

$$\bar{U}_i = \frac{1}{2} (b_{i+\frac{1}{2}} + b_{i-\frac{1}{2}}) = U_i \Delta x^{-2} \quad (A2)$$

$$A = C = -\Delta y^{-2} \quad (A3)$$

$$B = 2\Delta y^{-2} + 2(1-\mu_i) \bar{U}_i/\omega - \mu_{i-1} b_{i-\frac{1}{2}} \quad (A4)$$

$$D = (1-\mu_i) b_{i-\frac{1}{2}} - 2\mu_{i-1} \bar{U}_{i-1} \quad (A5)$$

$$E = \mu_{i-1} b_{i-\frac{3}{2}} \quad (A6)$$

$$\begin{aligned} \text{Where } \mu_i &= 0 \quad \text{if } U_i > 0 \\ &= 1 \quad \text{if } U_i \leq 0 \end{aligned} \quad (A7)$$

REFERENCES

1. Fedorenko, R.P.: A Relaxation Method for Solving Elliptic Difference Equations. USSR Computational Mathematics and Mathematical Physics, vol. 1, 1962, pp. 1092-1096.
2. Fedorenko, R.P.: The Speed of Convergence of One Iterative Process. USSR Computational Mathematics and Mathematical Physics, vol. 4, no. 3, 1964, pp. 227-235.
3. Bakhvalov, N.S.: On the Convergence of a Relaxation Method With Natural Constraints on the Elliptic Operator. USSR Computational Mathematics and Mathematical Physics, vol. 6, no. 5, 1966, pp. 101-135.
4. Brandt, Achi: Multi-Level Adaptive Technique (MLAT) For Fast Numerical Solution to Boundary Value Problems. Proceedings of the Third International Conference on Numerical Methods in Fluid Mechanics, vol. 1, 1972, pp. 82-89.
5. Brandt, Achi: Multi-Level Adaptive Techniques (MLAT). Part I. The Multi-Grid Method. IBM Report to be published.
6. Murman, E.M.: Analysis of Embedded Shock Waves Calculated by Relaxation Methods. Proceedings of AIAA Computational Fluid Dynamics Conference, Palm Springs, California, July 19-20, 1973, pp. 27-40.
7. Jameson, Antony: Transonic Potential Flow Calculations Using Conservation Form. Proceedings AIAA 2nd Computational Fluid Dynamics Conference, Hartford, Connecticut, June 19-20, 1975, pp. 148-161.

CONVERGENCE CRITERION FOR L1= 4 GRID IS EPS=1.783E-03

--NO STRETCH--
L= 1.00, D=6.250E-02

4	4.53EE+01	9 17	1.148E+01	5.457E-02	1.0	0
4	2.181E+01	3 17	6.239E+00	3.170E-02	2.0	0
PESCAL	L=4, RMAX	8.085E+00	RL2-	3.059E+00		
PESCAL	L=3, RMAX	2.619E+00	RL2-	1.489E+00		
PESCAL	L=2, RMAX	5.215E-01	RL2-	3.927E-01		
4	0.774E+00	23 17	1.026E+00	5.184E-03	4.6	0
4	1.931E+00	23 17	5.232E+01	2.874E-03	5.6	0
PESCAL	L=4, RMAX	7.216E-01	RL2-	2.496E-01		
PESCAL	L=3, RMAX	1.917E-01	RL2-	9.714E-02		
PESCAL	L=2, RMAX	2.410E-02	RL2-	1.456E-02		
4	4.043E-01	23 17	1.018E+01	4.691E-04	8.3	0
4	1.753E-01	23 17	4.521E-02	2.322E-04	9.3	0
4	3.351E-02	22 17	2.581E-02	1.392E-04	10.3	0
PESCAL	L=4, RMAX	3.563E-02	RL2-	1.352E-02		
PESCAL	L=3, RMAX	9.977E-03	RL2-	4.122E-02		
PESCAL	L=2, RMAX	2.228E-03	RL2-	1.311E-03		
4	2.147E-02	22 17	4.921E-03	2.450E-05	12.9	0
4	3.032E-03	21 17	2.914E-03	1.217E-05	13.9	0
4	4.645E-03	20 17	1.167E-03	7.044E-06	14.9	0

PLOT OF CPBAR FOR LEVEL 4

CSTAR=11.0 XINTERRUPTED

ORIGINAL PAGE IS
OF POOR QUALITY

Figure 1. - MG solution of Laplace's equation with smooth boundary conditions. 32 x 16 grid.

NODAL PREFERENCE CRITERION FOR L1= 5 GRID IS EPS=4.662E-04

X1= 2.00, DX=3.125E-02

NO. X-STRETCH
L= 1.00, Di=3.125E-02

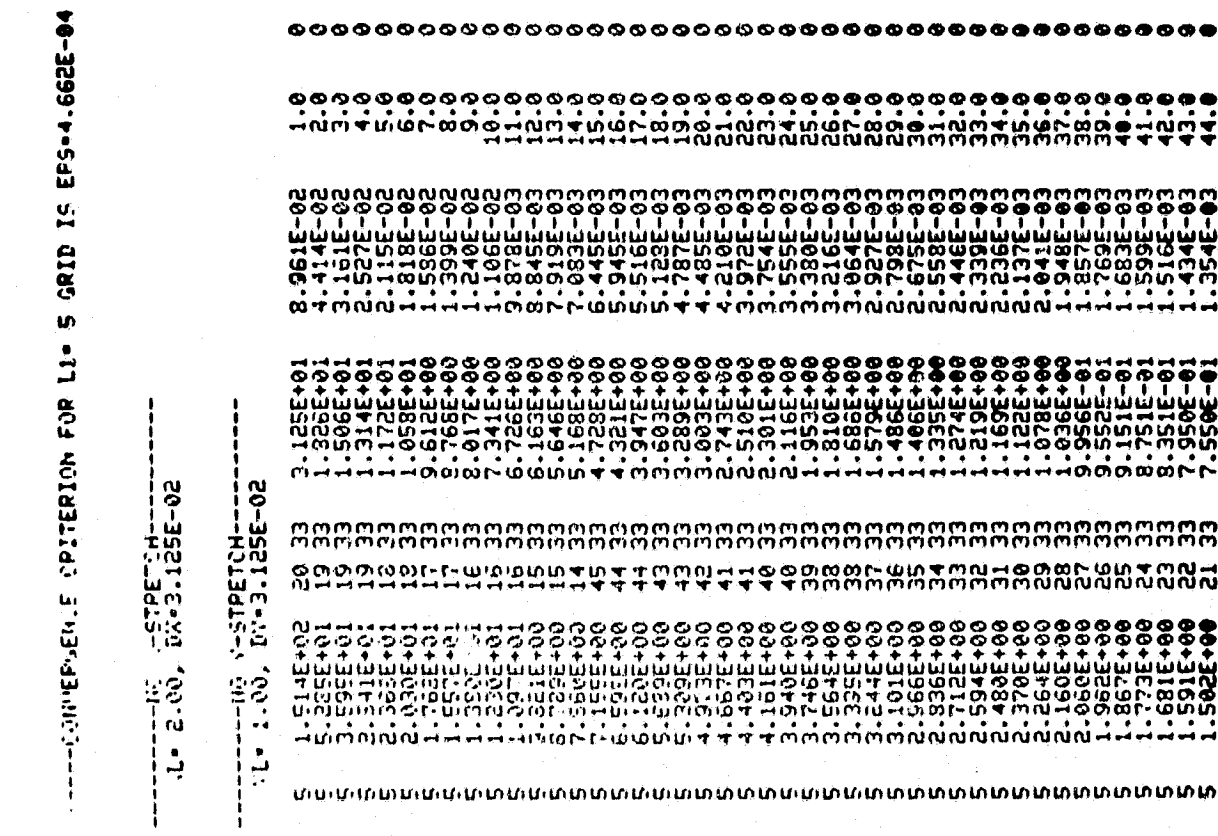
4. 042E-01	18	33	7.043E-02	1.230E-04	1.0	0	
5. 1.501E-01	17	33	3.685E-02	6.806E-05	2.0	0	
PESCAL.	L=4,	RMAX=	6.517E-02,	RL2=	1.715E-02		
PESCAL.	L=4,	RMAX=	1.912E-02,	RL2=	7.399E-03		
PESCAL.	L=3,	RMAX=	4.332E-03,	RL2=	2.409E-03		
PESCAL.	L=3,	RMAX=	7.393E-03,	RL2=	1.054E-05	4.6	0
PESCAL.	L=3,	RMAX=	1.933E-03,	RL2=	4.707E-06	5.6	0
PESCAL.	L=4,	RMAX=	4.829E-03,	RL2=	1.650E-03		
PESCAL.	L=4,	RMAX=	1.464E-03,	RL2=	8.060E-04		
PESCAL.	L=3,	RMAX=	7.393E-04,	RL2=	5.503E-04		
PESCAL.	L=2,	RMAX=	1.933E-04,	RL2=	1.751E-04		
PESCAL.	L=2,	RMAX=	4.637E-04	RL2=	1.531E-05	8.3	0
PESCAL.	L=3,	RMAX=	1.933E-04	RL2=	3.477E-07	9.3	0

PLUT OF CPBAR FOR LEVEL 5

CPSTAR=-1.000E+03

I I INTERRUPTED

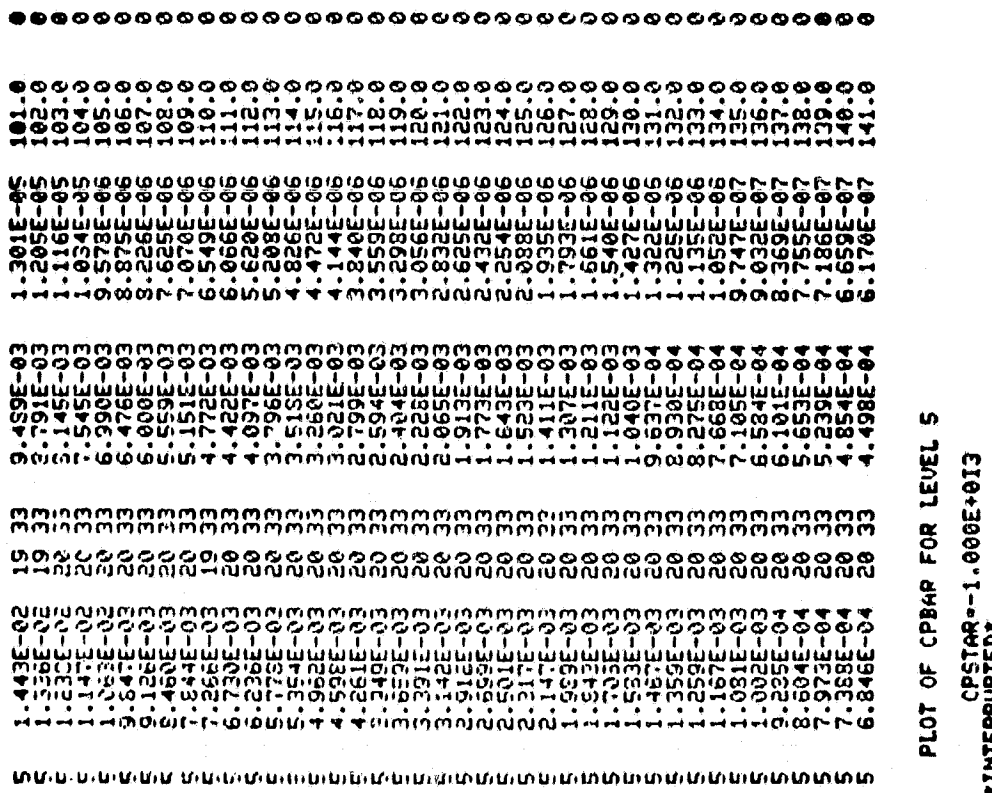
Figure 2. - MG solution of Laplace's equation with smooth boundary conditions. 64 x 32 grid, initialized by solution of figure 1.



45.0
 46.0
 47.0
 48.0
 49.0
 50.0
 51.0
 52.0
 53.0
 54.0
 55.0
 56.0
 57.0
 58.0
 59.0
 60.0
 61.0
 62.0
 63.0
 64.0
 65.0
 66.0
 67.0
 68.0
 69.0
 70.0
 71.0
 72.0
 73.0
 74.0
 75.0
 76.0
 77.0
 78.0
 79.0
 80.0
 81.0
 82.0
 83.0
 84.0
 85.0
 86.0
 87.0
 88.0
 89.0
 90.0
 91.0
 92.0
 93.0
 94.0
 95.0
 96.0
 97.0
 98.0
 99.0
 100.0

7.150E-01
 6.752E-01
 6.358E-01
 6.362E-01
 6.212E-01
 5.582E-01
 5.521E-01
 5.555E-01
 5.494E-01
 5.434E-01
 5.153E-01
 3.825E-01
 3.512E-01
 3.214E-01
 3.022E-01
 2.945E-01
 2.877E-01
 2.827E-01
 2.752E-01
 2.696E-01
 2.658E-01
 2.622E-01
 2.585E-01
 2.555E-01
 2.525E-01
 2.495E-01
 2.465E-01
 2.435E-01
 2.405E-01
 2.375E-01
 2.345E-01
 2.315E-01
 2.285E-01
 2.255E-01
 2.225E-01
 2.195E-01
 2.165E-01
 2.135E-01
 2.105E-01
 2.075E-01
 2.045E-01
 2.015E-01
 1.985E-01
 1.955E-01
 1.925E-01
 1.895E-01
 1.865E-01
 1.835E-01
 1.805E-01
 1.775E-01
 1.745E-01
 1.715E-01
 1.685E-01
 1.655E-01
 1.625E-01
 1.595E-01
 1.565E-01
 1.535E-01
 1.505E-01
 1.475E-01
 1.445E-01
 1.415E-01
 1.385E-01
 1.355E-01
 1.325E-01
 1.295E-01
 1.265E-01
 1.235E-01
 1.205E-01
 1.175E-01
 1.145E-01
 1.115E-01
 1.085E-01
 1.055E-01
 1.025E-01
 9.925E-02
 9.625E-02
 9.325E-02
 9.025E-02
 8.725E-02
 8.425E-02
 8.125E-02
 7.825E-02
 7.525E-02
 7.225E-02
 6.925E-02
 6.625E-02
 6.325E-02
 6.025E-02
 5.725E-02
 5.425E-02
 5.125E-02
 4.825E-02
 4.525E-02
 4.225E-02
 3.925E-02
 3.625E-02
 3.325E-02
 3.025E-02
 2.725E-02
 2.425E-02
 2.125E-02
 1.825E-02
 1.525E-02
 1.225E-02
 9.225E-03
 6.225E-03
 3.225E-03
 0.225E-03

Figure 3. - SLOR solution of Laplace's equation with smooth boundary conditions. 64 x 32 grid.
 (Continued)



ORIGINAL PAGE IS
OF POOR QUALITY

Figure 4. - MG solution of parabolic-arc airfoil. $N_\infty = 0.7$, $\tau = 0.1$, 64×32 grid.

No. "STRETCH"					
XL	DX	DL	DY	DX	DL
5 2.582E+02	17 33	1.934E+01	3.658E+02	1.0	0
5 3.369E+01	48 33	7.515E+00	1.982E+02	2.0	0
5 4.654E+01	47 33	5.935E+00	1.362E+02	3.0	0
5 3.105E+01	46 33	4.132E+00	1.644E+02	4.0	0
PESCAL. L=4, RMAX=	2.340E+01	RL2=	3.918E+00		
PESCAL. L=5, RMAX=	1.053E+01	RL2=	2.654E+00		
PESCAL. L=3, RMAX=	2.919E+01	RL2=	1.131E+00		
PESCAL. L=2, RMAX=	1.6 33	4.797E+01	7.600E+01	6.7	0
PESCAL. L=1, RMAX=	33 1.48	1.936E+01	4.398E+01	7.7	0
PESCAL. L=5, RMAX=	7.230E+01	RL2=	3.043E+01	8.7	0
PESCAL. L=4, RMAX=	2.332E+01	RL2=	8.356E+02		
PESCAL. L=3, RMAX=	7.744E+02	RL2=	3.357E+02		
PESCAL. L=2, RMAX=	1.914E+02	RL2=	1.003E+02		
PESCAL. L=1, RMAX=	1.6 33	2.275E+02	3.581E+05	11.4	0
PESCAL. L=5, RMAX=	4.9 33	1.021E+02	2.003E+05	12.4	0
PESCAL. L=4, RMAX=	49 33	6.139E+03	1.345E+05	13.4	0
PESCAL. L=3, RMAX=	2.290E+02	RL2=	9.966E+06	14.4	0
PESCAL. L=2, RMAX=	8.416E+03	RL2=	3.831E+03		
PESCAL. L=1, RMAX=	1.737E+03	RL2=	6.368E+04		
PESCAL. L=5, RMAX=	9.887E+03	49 33	8.715E+04	17.3	0
PESCAL. L=4, RMAX=	3.697E+03	6 33	3.332E+07	18.3	0

PLOT OF CPBAP FOR LEVEL 5

CPSTAR=81.673 *INTERRUPTED*

MINIMUM EPIFELION FOR L= 5 GRID IS EPS=4.662E-04

NO X-STRETCH		NO Y-STRETCH	
L	DY=3.125E-02	L	DY=1.451E-02
5	2.753E+02	17	33
5	3.596E+01	16	33
5	4.482E+01	49	33
5	2.919E+01	16	33
PESCAL.	L=5, PMAX=	2.088E+01,	RL2=
RESCL.	L=4, RMH=	9.996E+00,	RL2=
PESCAL.	L=3, PMAX=	2.871E+00,	RL2=
PESCAL.	L=2, PMAX=	1.633E+01	16
PESCAL.	L=1, PMAX=	4.581E+00	45
PESCAL.	L=0, PMAX=	2.562E+00	47
PESCAL.	L=-1, PMAX=	1.670E+00	49
PESCAL.	L=-2, PMAX=	1.420E+00	49
PESCAL.	L=-3, PMAX=	4.032E+01	7.971E-02
PESCAL.	L=-4, PMAX=	1.023E+00	40
PESCAL.	L=-5, PMAX=	1.352E+01	45
PESCAL.	L=-6, PMAX=	9.050E+02	49
PESCAL.	L=-7, 234E-02	49	33
PESCAL.	L=-8, PMAX=	5.714E+02	RL2=
RESCL.	L=4, RMH=	1.174E+02,	RL2=
RESCL.	L=3, PMAX=	4.874E+03,	RL2=
RESCL.	L=2, 454E-02	41	32
RESCL.	L=1, 248E-03	41	32
RESCL.	L=0, 3666E-03	41	32

PLOT OF CPBAR

Figure 5. - MG solution of parabolic-arc airfoil. $M_\infty = 0.85$, $\tau = 0.1$, 64×32 grid.

-----CINNEPGENE : FITTERION FOR L1, S GPID IS EPS=4.662E-04

:L= 2.00, DX=3.125E-02

-----NO %STRETCH-----

:L= 2.00, BY=6.250E-02

-----CINNEPGENE : FITTERION FOR L1, S GPID IS EPS=4.662E-04

:L= 2.00, BY=6.250E-02

PLOT OF CIPER FOR LEVE

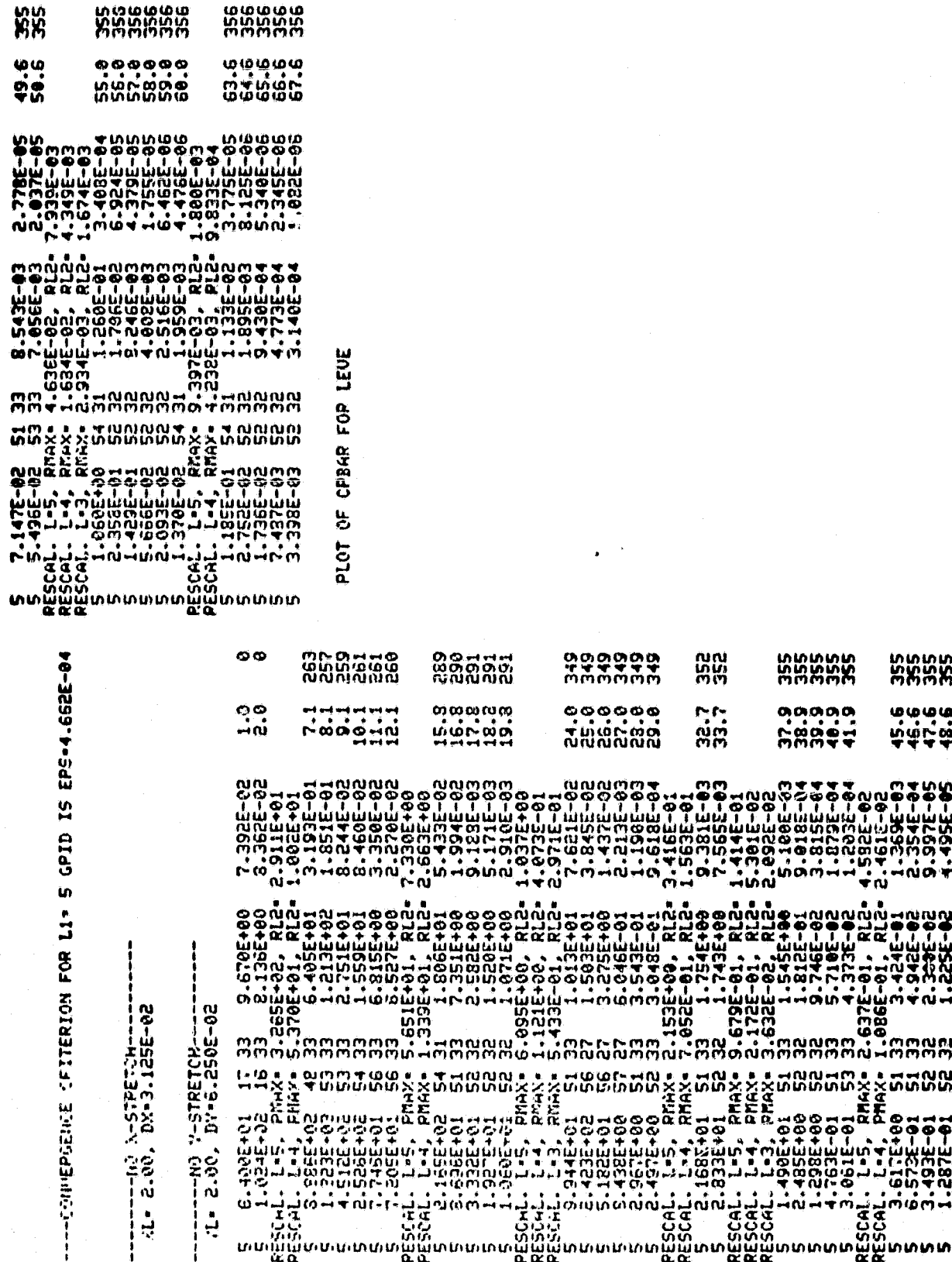


Figure 6. - MG solution of parabolic-arc airfoil. $M_\infty = 0.95$, $\tau = 0.1$, 64×32 grid.

ORIGINAL PAGE
OF POOR QUALITY

Y- ⁻ STRETCH FUNCTIONS-----						
I	Y-	SX(I)	SXH(I,			
2	-3.346	3.309E-02	5.668E-02			
33	0.300	6.199E-01	6.189E-01			
J	Y-	22(J)	SY(J)	SYH(J)		
2	1.553	3.346	.082	.122		
33	0.300	0.086	1.334	1.333		
PESCAL.	L-5, RMAX=	1.594E+02	24.33	1.709E+01	1.462E+01	1.0
PESCAL.	L-4, RMAX=	1.655E+01	23.33	5.191E+00	1.727E+01	2.0
PESCAL.	L-3, RMAX=	1.860E+02	42.33	1.708E+01	1.584E+01	3.0
PESCAL.	L-2, RMAX=	1.860E+02	46.32	2.801E+01	6.949E+02	4.0
PESCAL.	L-1, RMAX=	2.795E+01	41.32	7.625E+00	3.740E+02	5.0
PESCAL.	L-0, RMAX=	2.795E+01	41.32	2.454E+00	1.601E+02	6.0
PESCAL.	L-5, RMAX=	1.373E+01	46	32.1.823E+00	1.893E+02	7.0
PESCAL.	L-4, RMAX=	1.058E+01		1.605E+00	1.605E+02	
PESCAL.	L-3, RMAX=	2.451E+00		7.702E+01	7.702E+02	
PESCAL.	L-2, RMAX=	1.065E+00		4.303E+01	6.239E+02	
PESCAL.	L-1, RMAX=	4.729E+01	41	33.7.852E+00	11.5.596	57
PESCAL.	L-0, RMAX=	5.541E+00	54	5.9.560E+01	13.5.581	57
PESCAL.	L-5, RMAX=	2.373E+00	55	5.2.404E+01	9.294E+02	57
PESCAL.	L-4, RMAX=	5.9.386E+01	54	3.1.826E+01	7.223E+03	583
PESCAL.	L-3, RMAX=	8.616E+01	41	3.7.852E+00	1.749E+02	583
PESCAL.	L-2, RMAX=	4.822E+01		1.569E+01	1.443E+02	583
PESCAL.	L-1, RMAX=	2.475E+01	55	9.2.446E+00	9.443E+02	583
PESCAL.	L-0, RMAX=	1.381E+01	55	9.1.681E+00	4.465E+02	583
PESCAL.	L-5, RMAX=	1.825E+00	55	9.1.552E+01	6.989E+02	583
PESCAL.	L-4, RMAX=	3.410E+01	55	13.7.922E+02	4.565E+03	583
PESCAL.	L-3, RMAX=	2.615E+01	23	33.6.413E+02	3.568E+03	583
PESCAL.	L-2, RMAX=	4.717E+01		6.145E+01	2.312E+02	583
PESCAL.	L-1, RMAX=	1.568E+01		1.528E+01	1.298E+02	583
PESCAL.	L-0, RMAX=	7.464E+02		5.728E+02	5.728E+02	583
PESCAL.	L-5, RMAX=	8.633E+02		4.628E+02	2.427E+02	583
PESCAL.	L-4, RMAX=	2.327E+02		2.105E+02	2.210E+03	583
PESCAL.	L-3, RMAX=	1.375E+01	57	8.1.451E+00	1.1.298E+01	583
PESCAL.	L-2, RMAX=	1.197E+01	58	4.7.928E+01	1.416E+02	583
PESCAL.	L-1, RMAX=	2.089E+00	58	4.1.259E+01	1.617E+02	583
PESCAL.	L-0, RMAX=	3.088E+01	58	6.4.661E+01	2.243E+03	583
PESCAL.	L-5, RMAX=	4.475E+01	56	13.4.273E+02	1.414E+03	583
PESCAL.	L-4, RMAX=	3.364E+01	55	25.3.692E+02	1.819E+03	583
PESCAL.	L-3, RMAX=	1.494E+01		2.556E+02	6.633E+02	583
PESCAL.	L-2, RMAX=	1.374E+01		2.556E+02	1.865E+02	583
PESCAL.	L-1, RMAX=	6.633E+02		RL2- 1.465E+03	RL2- 6.633E+02	583
PESCAL.	L-0, RMAX=	7.7.765E+02		RL2- 1.465E+03	RL2- 7.765E+02	583

Figure 7. - MG solution of parabolic-arc airfoil. $M_{\infty} = 0.95$, $\tau = 0.1$, 64×32 stretched grid.

(Continued)

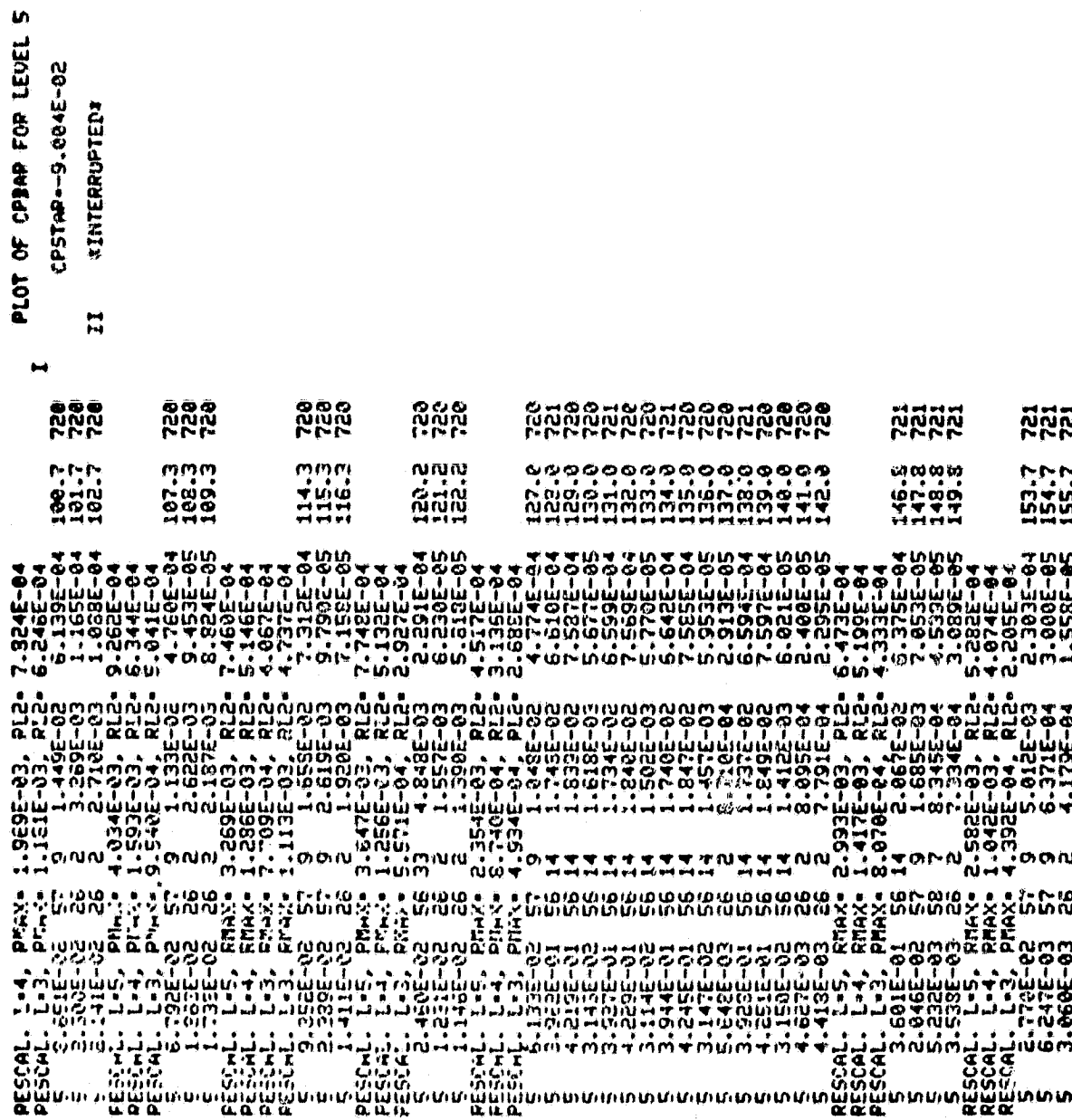


Figure 7. - Concluded.

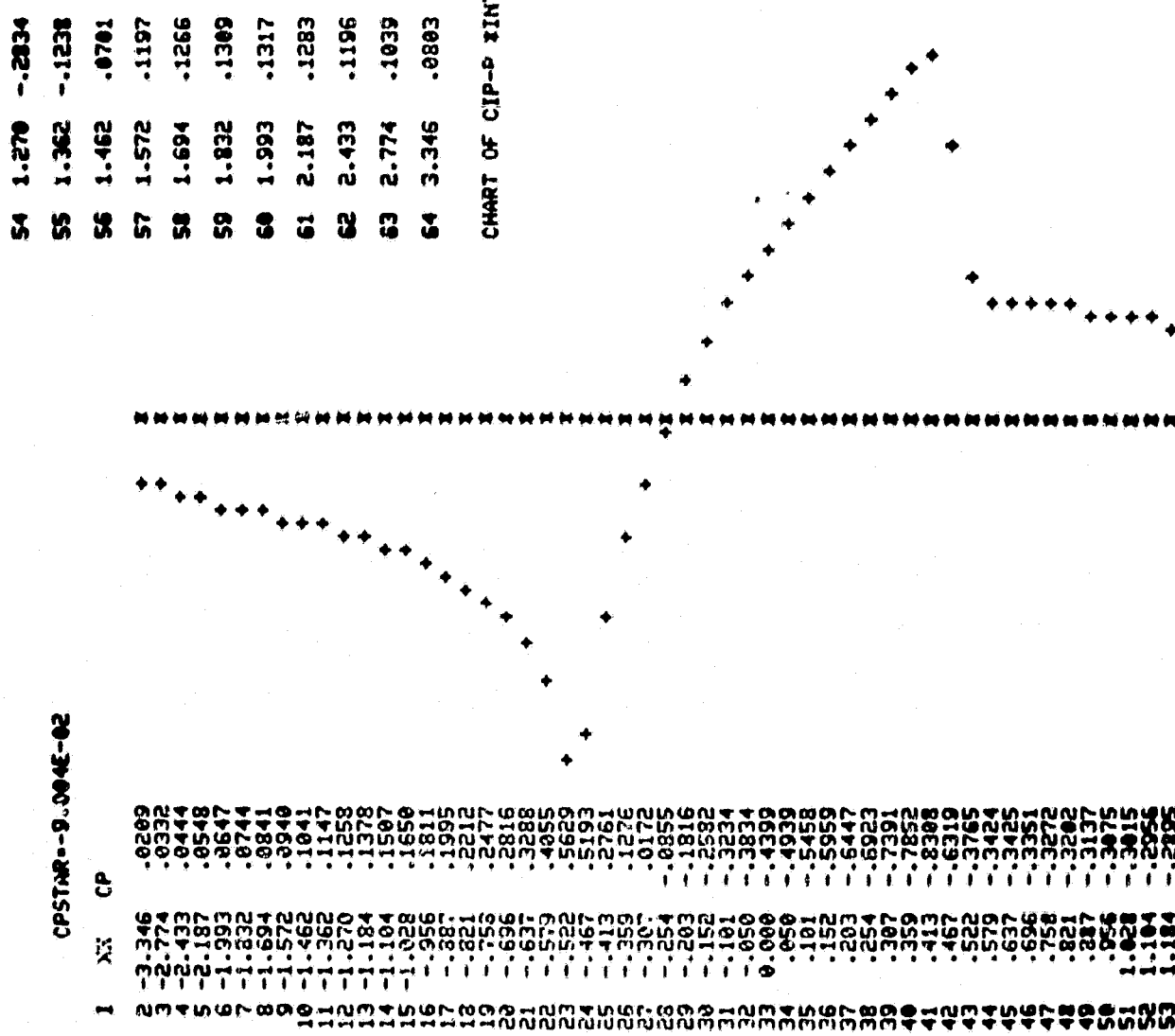


Figure 8. - Pressure distribution along $y = 0$ for solution of figure 7.

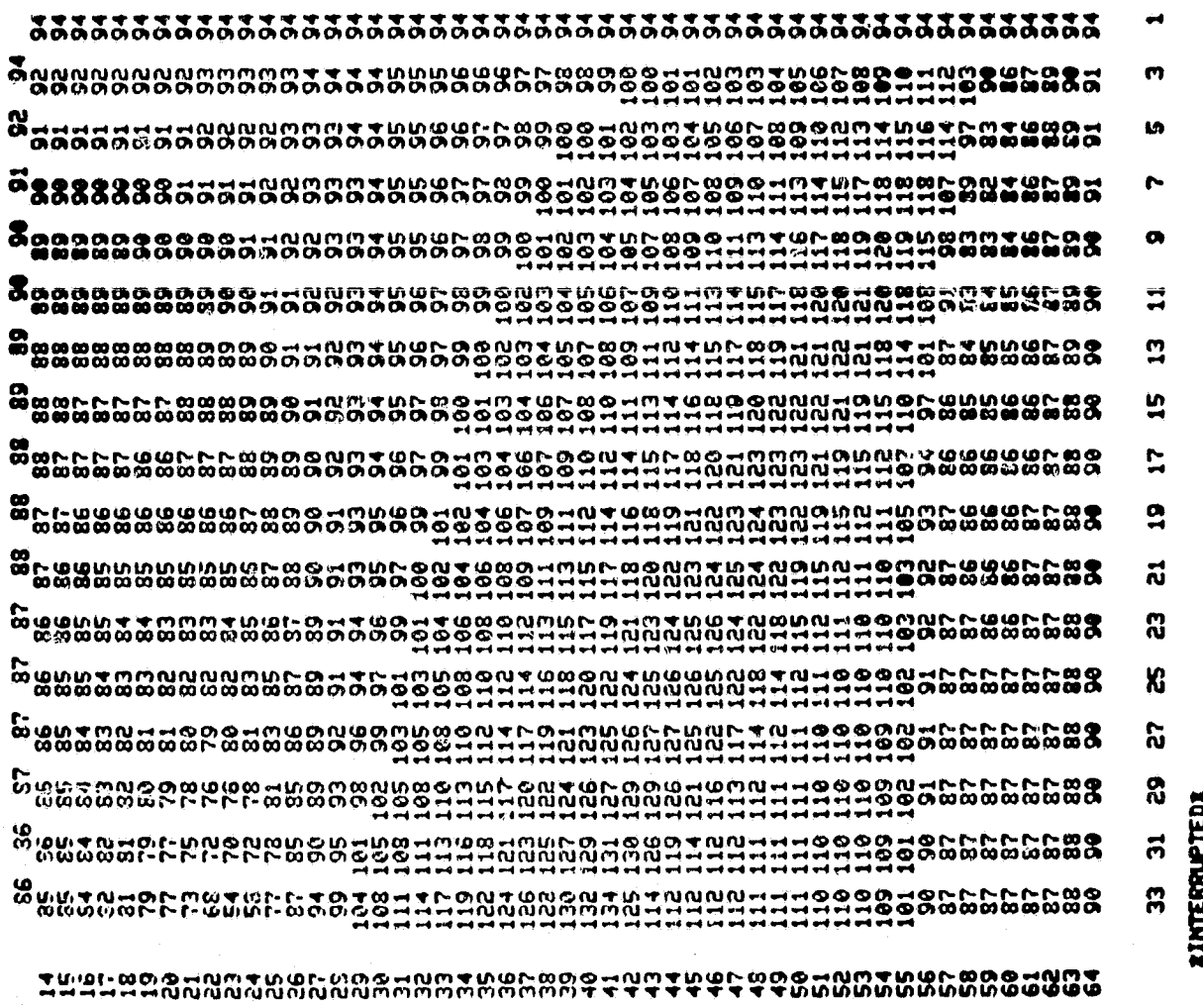


Figure 9. - Mach number chart for solution of figure 7.

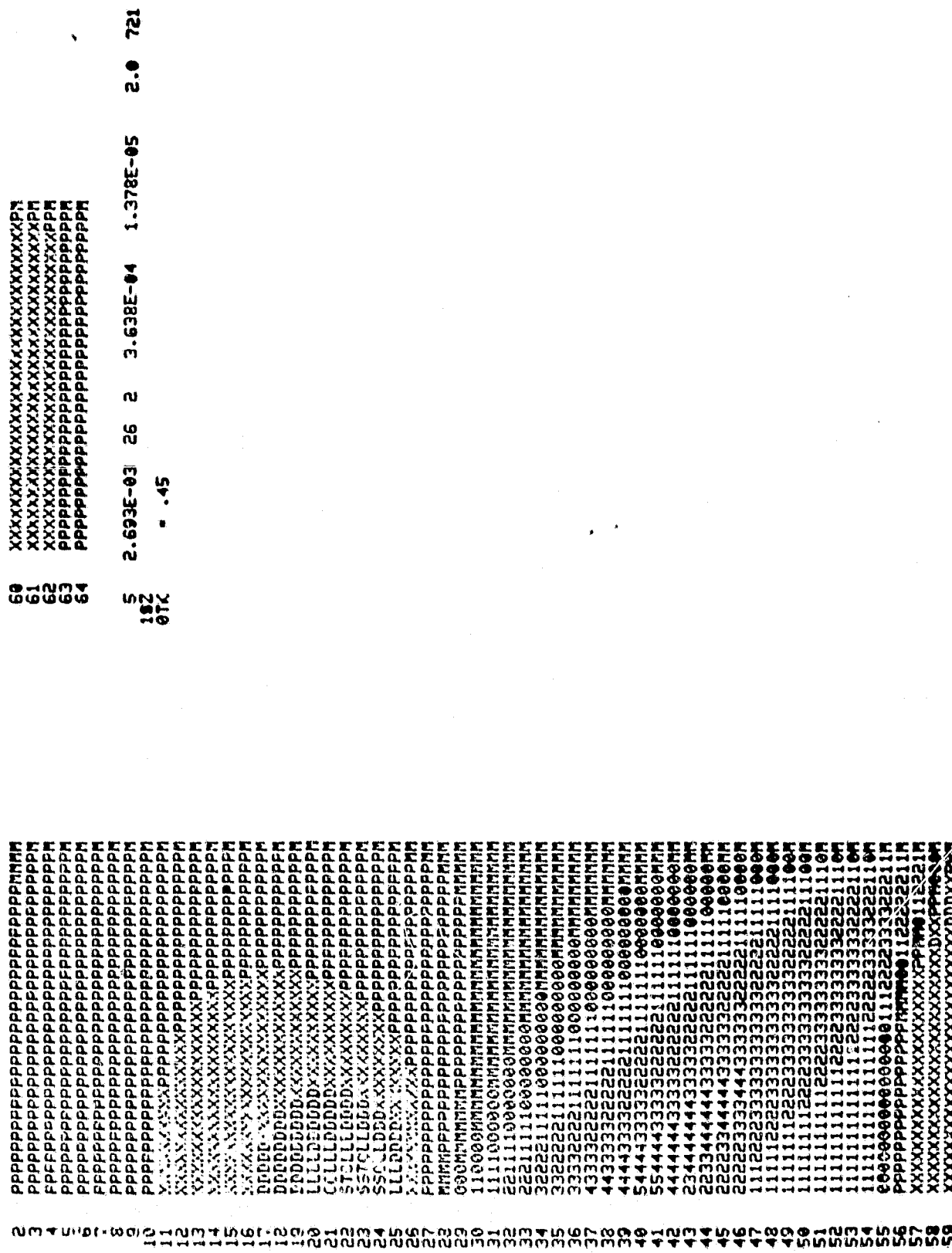


Figure 10. - Isobar chart for solution of figure 7.

SUMMARY OF MULTIGRID RESULTS
 64 X 32 CELLS

PROBLEM DESCRIPTION		*EFFECTIVE SPECTRAL RADIUS	
		MG	SLOR
UNSTRETCHED GRID	LAPLACE'S Eq., Smooth B.C.'s	.583	,924
	PARABOLIC AIRFOIL, $M_\infty = .70$.549	.858
	" " .85	.593	.855
	" " .95	.358	.957
	" " .95	.335	.974
	STRETCHED GRID		

* EFF. SPEC. RAD. = (FINAL ERROR/INITIAL ERROR) $^{1/2}$ (WORK UNITS)

FIGURE 11. - SUMMARY OF MULTIGRID RESULTS.